Shallow Water Equations
Laplace Transform Integration

Pieters Michael and Ysebaert Tess

December 9, 2016

1 Shallow Water Equations

The shallow water equations are a set of hyperbolic partial differential equations that model the propagation of disturbances in water and other incompressible fluids. The one dimensional form was derived by the Frenchman Adhémar Jean Claude Barré de Saint-Vernat, which until this day is still actively used in hydraulic engineering. A fluid is considered shallow when the depth of the fluid is small compared to the wave length of the disturbance. This means that this set of equations provides a reasonable way to model for example Tsunami waves, which can reach considerable heights. Additionally this set of equations have been applied for atmospheric flows, storm surges, flows around structures and planetary flows.

We shall assume that the fluid is so shallow that the flow velocity U can be considered constant with depth. At the free surface, located at height H, pressure p is equal to atmospheric pressure p_0 and is also assumed constant and uniform.

This type of flow is governed by an **equation of motion**:

$$\frac{\partial u}{\partial t} + U\frac{\partial u}{\partial x} + g\frac{\partial h}{\partial x} = 0 \tag{1}$$

and an **equation of continuity**:

$$\frac{\partial h}{\partial t} + H\frac{\partial u}{\partial x} + U\frac{\partial h}{\partial x} = 0 \tag{2}$$

Suppose now that the shallow water system is motionless ($U = 0$), and we perturb the system, such that $u(x,t) = u^{'}(x,t)$ and $h(x,t) = H + h^{'}(x,t)$, we will retrieve a set of wave equations:

$$\begin{aligned} \frac{\partial^2 u^{'}}{\partial t^2} - gH\frac{\partial^2 u^{'}}{\partial x^2} &= 0 \\ \frac{\partial^2 h^{'}}{\partial t^2} - gH\frac{\partial^2 h^{'}}{\partial x^2} &= 0 \end{aligned} \tag{3}$$

These describe the motion of gravity shallow water waves which have a phase speed $c_p = \sqrt{gH}$.

2 Numerical implementation

To numerically solve the set of equations (1) and (2), we follow the same method as developed by Clancy and Lynch (2011). We first decompose $u(x,t)$ and $h(x,t)$ in harmonic functions:

$$\begin{aligned} u(x,t) &= \sum_{k=-K_{max}}^{K_{max}} u_k(t) \exp ikx \\ h(x,t) &= \sum_{k=-K_{max}}^{K_{max}} h_k(t) \exp ikx \end{aligned} \tag{4}$$

where $u_k(t)$ and $h_k(t)$ are time-dependent spectral coefficients that can be determined with a Fast Fourier Transform for all wavenumbers whose magnitude is smaller than the Nyquist wavenumber K_{max}.

Plugging these Fourier expansions into the original set of shallow water equations, gives us a set of differential equations that govern the time evolution of these spectral coefficients.

$$\begin{aligned} \frac{du_k(t)}{dt} + iUku_k(t) + igkh_k(t) = 0 \\ \frac{dh_k(t)}{dt} + iUku_k(t) + igkh_k(t) = 0 \end{aligned} \tag{5}$$

To determine this time evolution, a Laplace transform integration is performed, which transforms (5) from the time-domain to the complex s-plane.

$$\begin{aligned} s\hat{u}_k(s) - u_k^{n-1} + iUk\hat{u}_k(s) + igk\hat{h}_k(s) = 0 \\ s\hat{h}_k(s) - h_k^{n-1} + iHk\hat{u}_k(s) + iUk\hat{h}_k(s) = 0 \end{aligned} \tag{6}$$

This gives us a relationship between the Laplace transformed spectral coefficients $\hat{u}_k(s)$ and $\hat{h}_k(s)$, and the spectral coefficients u_k^{n-1} and h_k^{n-1}, which are known values and were determined from a previous time step. The solution for (6) given in matrix notation:

$$\begin{bmatrix} \hat{u}_k(s) \\ \hat{h}_k(s) \end{bmatrix} = \frac{\begin{bmatrix} s+iUk & -igk \\ -iHk & s+iUk \end{bmatrix}}{(s+iUk)^2 + gHk^2} \begin{bmatrix} u_k^{n-1} \\ h_k^{n-1} \end{bmatrix} \tag{7}$$

Applying an inverse Laplace transformation will determine the spectral coefficients u_k^n and h_k^n of the current time step. Since Laplace transformations are used, the possibility exists to filter out unwanted high frequencies by applying a filter in the complex domain. This is accomplished by integrating over a circle centered in the origin with radius γ, when performing an inverse Laplace transformation. This inversion is done numerically by summation over a N-sided polygon. To ensure that the frequencies are damped without phase shift, N is taken as a multiple of 4.

The numerical inverse Laplace transformation is determined as follows:

$$\begin{aligned} u_k^n &= L_n^*[\hat{u}_k(s)]|_{t=t_{n-1}+\Delta t} = \frac{1}{N}\sum_{j=1}^{N} s_j \hat{u}_k(s_j) \exp s_j \Delta t \\ h_k^n &= L_n^*[\hat{h}_k(s)]|_{t=t_{n-1}+\Delta t} = \frac{1}{N}\sum_{j=1}^{N} s_j \hat{h}_k(s_j) \exp s_j \Delta t \end{aligned} \tag{8}$$

Instead of using an upward scheme (8) where the spectral coefficients are determined from t_{n-1} to t_n, one can also utilize a centered scheme where the value of the fields are determined at t_{n+1} with information at t_{n-1}:

$$\begin{aligned} u_k^{n+1} &= L_n^*[\hat{u}_k(s)]|_{t=t_{n-1}+2\Delta t} = \frac{1}{N}\sum_{j=1}^{N} s_j \hat{u}_k(s_j) \exp s_j 2\Delta t \\ h_k^{n+1} &= L_n^*[\hat{h}_k(s)]|_{t=t_{n-1}+2\Delta t} = \frac{1}{N}\sum_{j=1}^{N} s_j \hat{h}_k(s_j) \exp s_j 2\Delta t \end{aligned} \tag{9}$$

Our numerical scheme will make use of a Leapfrog time-stepping method where an upward scheme (8) is used for calculating the field values after the first time step. Then a centered scheme (9) is applied during the remainder of the simulation.

2.1 Benchmark Result

To benchmark our numerical scheme, we will do an initial comparison with the Semi-Implicit Spectral method. A grid of 100 points is used along the spatial domain with a discretization parameter $\Delta x = 1$. For the Laplace Transform method 16 vertices are used when performing the inverse Laplace transformation. A contour radius of $\gamma = 2$ is taken.

The initial height of the fluid is taken as a Bell-shaped function:

$$h = 1 + \frac{2}{5} \exp\big[-50(x - 0.5)^2 \big] \tag{10}$$

The advection speed of the fluid is set at $U = 1$.

A low and high time-resolution simulation ($\Delta t = 1$ and $\Delta t = 0.1$) are done for both types of schemes. The simulations are run for a total time of 100 time units. The numerical results for $t = 20$, $t = 40$, $t = 80$ and $t = 100$ are displayed in the Figures (1) and (2).

The Laplace Transform method is far more accurate than the Semi-Implicit Spectral scheme. There is not that much accuracy gain for the former method if you select a smaller time step. That is one of the main advantages of the Laplace Transform technique: it converges much faster to an accurate solution; enabling the use of higher time steps. In comparison, the spectral method actually performs quite poorly if one looks at the low time-resolution simulation.

One can also notice that the numerical results obtained with the Laplace Transform method are slightly damped. As already mentioned, a filter is applied in the complex domain which will nevertheless damp all frequencies to a certain degree.

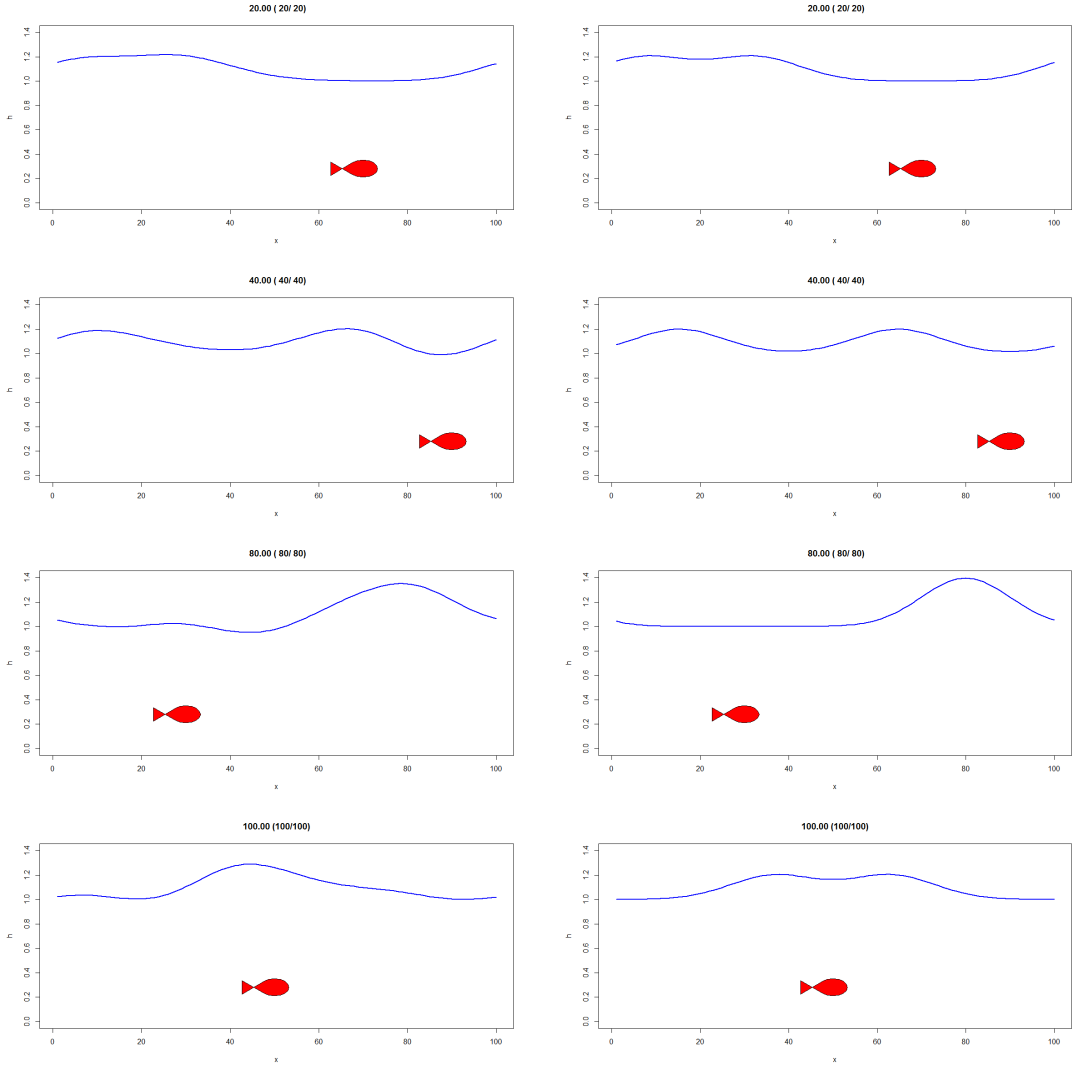

Figure 1: Low resolution simulation ($\Delta t = 1$): solutions at $t = 20$, $t = 40$, $t = 80$ and $t = 100$ for the Semi-Implicit Spectral scheme (Left) and the Laplace Transform Method (Right)

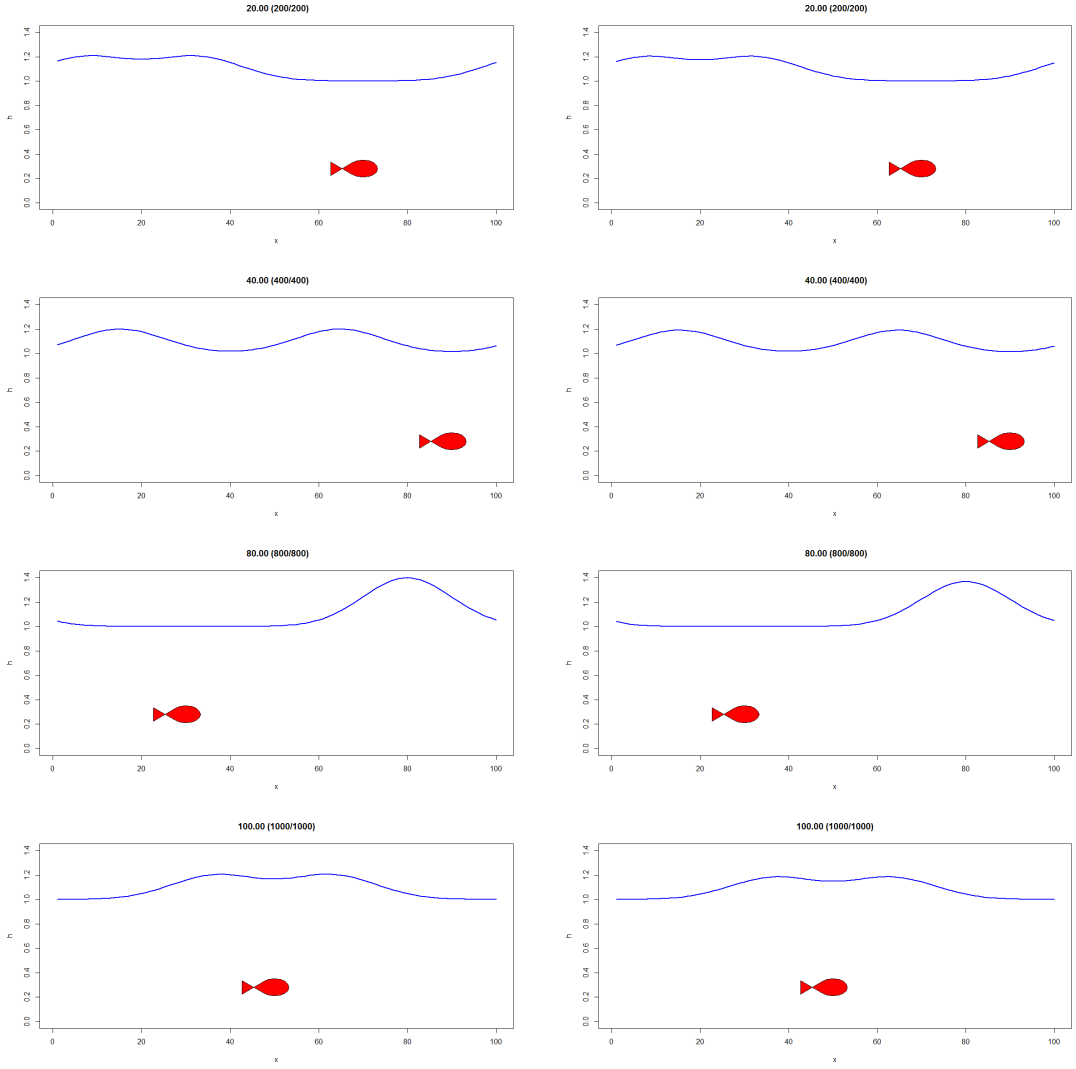

Figure 2: High resolution simulation ($\Delta t = 0.1$): solutions at $t = 20$, $t = 40$, $t = 80$ and $t = 100$ for the Semi Implicit Spectral scheme (Left) and the Laplace Transform Method (Right)

3 Application of the Laplace transformation

3.1 Filtering time-stepping scheme

The modified inversion of the Laplace transform has the property of eliminating the high frequency wave components, as such acting as a filtering time-stepping scheme. The numerical operator used for the modified inversion damps waves with a speed larger than the radius of the circumscribed N-sided polygon, i.e. falling outside the polygon. At the same time, it truncates the original harmonic wave to N terms. In case of the shallow water equations, there exists two wave solutions, one wave traveling to the left at the advection speed minus the speed of the gravity wave and one wave traveling to the right at the advection speed plus the speed of the gravity wave. The Laplace transformed shallow water equation has two simple poles on the imaginary axis, which represent the speed of the two wave solutions. At a zero advection speed, the two poles are at an equal distance from the origin with a negative value and a positive value for the left and right traveling wave, respectively. However, with a non-zero, positive advection speed, the two poles shift upwards on the imaginary axis.

It is demonstrated that with every time step, waves are damped by the same constant value, determined by the response function H_N:

$$H_N(\omega) = \frac{1}{1 + (\frac{i\omega}{\gamma})^N} \tag{11}$$

Plotting the response function (11) as a function of its argument $\frac{\omega}{\gamma}$, shows the amount of damping with respect to wave frequency. After a certain amount of time all frequencies, regardless of N, will be completely damped. The amount of damping is influenced by both the radius and the number of edges of the N-sided polygon. Lowering the radius will increase the amount of wave frequencies that will be damped rapidly. Increasing N will make the response function more step-like with a clear defined cut-off at $\omega = \gamma$.

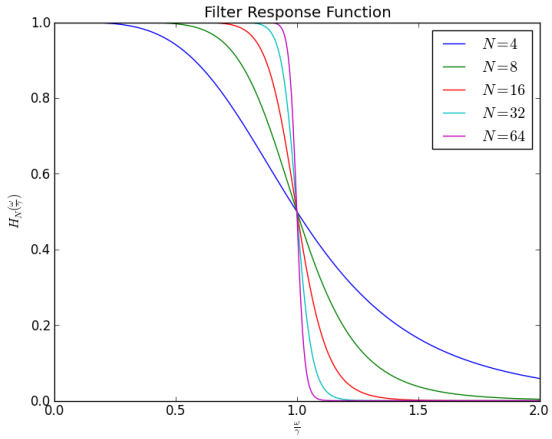

Figure 3: Filter response function for several values of N

Waves with a frequency ω equal to the radius γ, will be damped by half their amplitude after every time step. To display this damping, we will initialize the height of the fluid according to a harmonic function with a single wavenumber k.

The choice of this particular k can be determined with the aid of the dispersion relation $\omega = \left[U \pm \sqrt{gH}\right]]k$. In our numerical scheme a parameter α is introduced to set the wavenumber k and thus the frequency ω of the harmonic function. This is done according to the following relationship:

$$\alpha = \frac{Lk}{2\pi} = \frac{L\omega}{2\pi\sqrt{gH}} \tag{12}$$

Using the following values $L = 400$, $H = 1$, $U = 0$, $\omega = 1$ and $\gamma = 1$, gives an α of approximately 20. Thus, for this particular value of α, the waves are damped by half their amplitude with every time step.

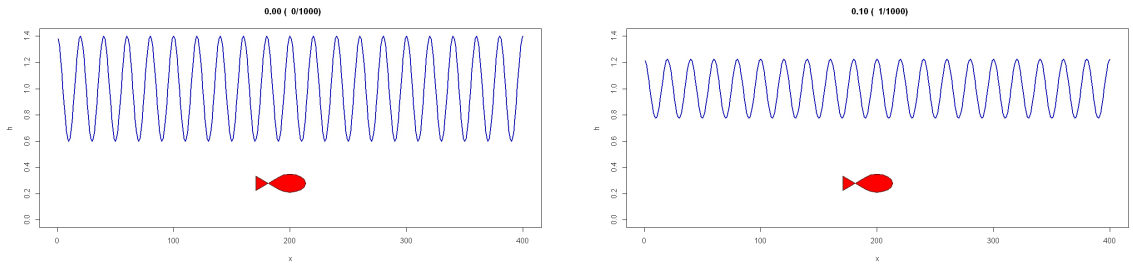

Figure 4: Harmonic function at $t = 0$ (Left) and at $t = 1$ (Right)

Figure (4) shows that the amplitude of the harmonic function decreases from 0.4 to 0.2 after one time step, as was expected.

To demonstrate how the numerical scheme can filter out certain frequencies, we consider a superposition of two harmonic waves with $\alpha = 2$ and $\alpha = 30$. Only the lowest frequency lies within the cut-off radius of the contour polygon. As time goes on, the highest frequency is gradually getting damped out. The benefit is that by selecting a good cut-off radius, we can damp out unwanted frequencies, that might not be physically interesting in the system that we study, but that otherwise could put serious time constraints on the stability.

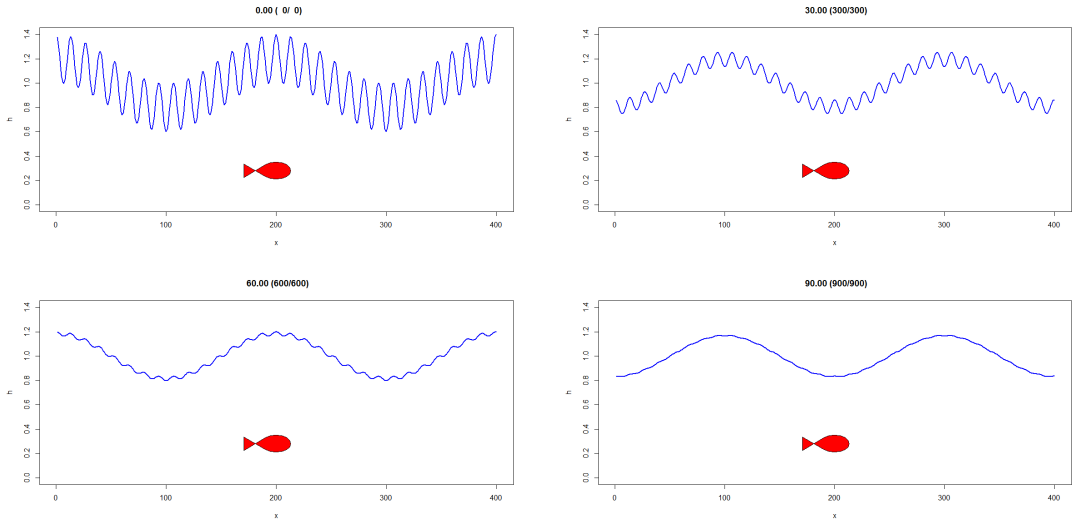

Figure 5: Numerical solution at $t = 0$, $t = 30$, $t = 60$ and $t = 90$

According to (11), there will be no damping for waves with frequency $\omega = 0$. This can happen when the magnitude of the advection speed is equal to one of the characteristic speeds of the system, or in this case the speed of the gravity shallow water waves ($U = \pm\sqrt{gH}$). In this particular case there will be no damping for any wavenumbers.

To highlight this, we use a very sharp defined filter in the contour plane ($N = 32$) with a very small contour radius $\gamma = 0.1$. We initialize harmonic waves with a mean height $H = 1$ and an amplitude $H_m = 0.4$ for different wavenumbers $\alpha = 30$ and $\alpha = 60$. When the simulation is run for 1000 time units ($\Delta x = 0.1$), the amplitudes of these waves will not change. See Figure (6)

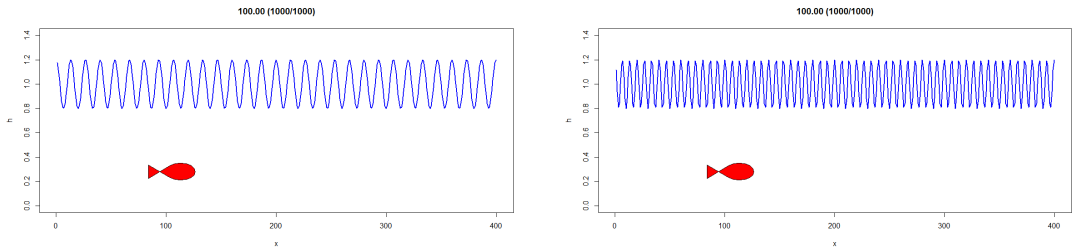

Figure 6: Numerical solution for $\alpha = 30$ and $\alpha = 60$ with $U = 3.13209195267$

3.2 Stability

The integral in the inverse Laplace is approximated by a sum, which introduces an error. Lynch (1986) determined a stability criterion for the maximum allowable timestep:

$$\Delta t \leq \frac{(N!)^{\frac{1}{N}}}{2\gamma} \tag{13}$$

This is a very lenient stability criterion, as it does not depend on the spatial resolution. This is the case for the Courant-Friedrichs-Lewy criterion; if the spatial resolution is increased, the temporal resolution must also be increased to maintain stability, and, thus the computational demand would increase substantially. The stability of our model is only dependent on the number of edges of the polygon and its radius. Both values are set by the modelers, allowing to have stability at all times. The maximum radius and maximum timestep at which stability is ensured, can be calculated.

From our experiments, this stability criterion was only valid for runs with a zero advection speed. Runs with a non-zero advection speed became instable after a certain amount of time, indicating that the spatial resoltion does play a role in determing stability.

4 References

1. Colm Clancy & Peter Lynch, *Laplace transform integration of the shallow-water equations. Part I: Eulerian formulation and Kelvin waves*, Quaterly Journal of the Royal Meteorological Society, 2011

2. Peter Lynch, *Numerical forecasting Laplace transforms: Theory and application to data assimilation*, Technical Note No.48, Meterology Service, 1986

3. Jaan Kiusalaas, *Numerical Methods in Engineering with Python*, 2nd edition, 2010

4. Mark Newman, *Computational Physics*, 1st edition, 2012

5. Steven Smith, *The scientist and Engineer's guide to Digital Signal processing*, 2nd edition, 1999